MINERALOGICAL MAGAZINE, DECEMBER 1985, VOL. 49, PP. 671–81

Pb–Zn and minor U mineralization at Tyndrum, Scotland

RICHARD A. D. PATTRICK

Department of Geology, University of Manchester, Manchester M13 9PL

ABSTRACT. The Tyndrum Pb–Zn mineralization occurs as veins and vein breccias in NE–SW trending fractures associated with the Tyndrum–Glen-Fyne fault. The major minerals are quartz, galena, and sphalerite with minor chalcopyrite and baryte. Tetrahedrite (sometimes silver- and cadmium-rich), pyrargyrite, marcasite, and pyrite occur as small inclusions (< 100 μm) in the galena-rich veins. Sphalerite formed early in the depositional sequence, mainly in breccias, with increasing amounts of galena and chalcopyrite deposited in the later vein stages of mineralization. Uraniferous veins post-date the main Pb–Zn mineralization and contain uraninite, calcite, baryte, galena, sphalerite, chalcopyrite, argentite, chalcocite, tetrahedrite, and safflorite.

Fluid inclusion studies reveal that the mineralizing solutions contained *c.*20 wt. % equivalent NaCl + KCl, had an Na/K ratio of 3 : 1 and were boiling during mineral precipitation.

The Tyndrum fault controlled the upward flow of the hydrothermal solutions and its intersection with fractures in quartzites favoured the siting of the veins. The depositional sequence is explained by an increase in temperature during the mineralizing episode. The uraniferous veins may be a late oxidized stage of the main Pb–Zn mineralization.

KEYWORDS: Pb–Zn mineralization, uranium veins, Tyndrum, Scotland, fluid inclusions.

THE Tyndrum mineralization is a series of base-metal veins hosted by Dalradian metasediments situated in the Central Highlands of Scotland. The veins were discovered in 1741 and worked until 1862. The dumps were reworked between 1916 and 1925 when a level was driven into a fault plane in the Tyndrum Main Mine. Most of the 20 000 tons of high grade (*c.*30%) Pb–Zn ore came from the Main Mine (fig. 1).

Previous descriptions of the Pb–Zn mineralization were by Odernheimer (1841), Thost (1860), Wilson and Cadell (1884), Wilson and Flett (1921), and a mineralogical investigation was carried out by Pattrick (1981). Brief descriptions of the late U–Cu stage of mineralization are given by Harrison (1956) and Darnley *et al.* (1960).

The vein mineralization at Tyndrum occupies NE–SW trending fractures which are sub-parallel to the Tyndrum–Glen-Fyne fault and is best developed in meta-psammitic rocks of the Grampian Group to the west of this fault. To the east of the fault and south of Eas Anie (fig. 1) the strata are largely Argyll Group schists. The mineralized localities described in Wilson and Flett (1921) and Pattrick (1981) are shown in fig. 1. In the Tyndrum Main Mine the mineralization is mainly confined to a fracture dipping *c.*75° southeast (the 'Hard Vein') which terminates against the Tyndrum fault (the 'Clay Vein'); the latter is one of the NE–SW trending Lower Devonian sinstral strike-slip faults that are parallel to the Great Glen fault and postdate the late Caledonian granites.

The veins were heavily worked and little *in situ* material remains, thus the mineralogy is largely described from dump samples.

The mineralogy of the Pb–Zn ore in the Tyndrum Main Mine

Ore types. The dump samples comprise two main ore types; breccia-ores and vein-ores. The breccia-ores consist of angular fragments of quartzite surrounded by acicular quartz and later sphalerite and/or galena. Vugs rimmed by euhedral quartz are a common feature of the breccias. Some are hydraulic breccias in which the quartzite fragments (1–20 cm across) have moved relatively little with respect to each other. Other samples resemble injection breccias with the quartzite fragments (usually < 3 cm) well separated and randomly orientated; in these breccias there is little evidence of rounding due to abrasion but significant replacement of the quartzite fragments by cryptocrystalline silica.

The vein-ores exhibit successive mineral growth perpendicular to the vein walls. One distinct type of vein-ore comprises massive galena (< 60 cm in width) with inclusions of chalcopyrite and fragments of earlier quartz and sphalerite. This ore was termed 'Steel Ore' by the miners.

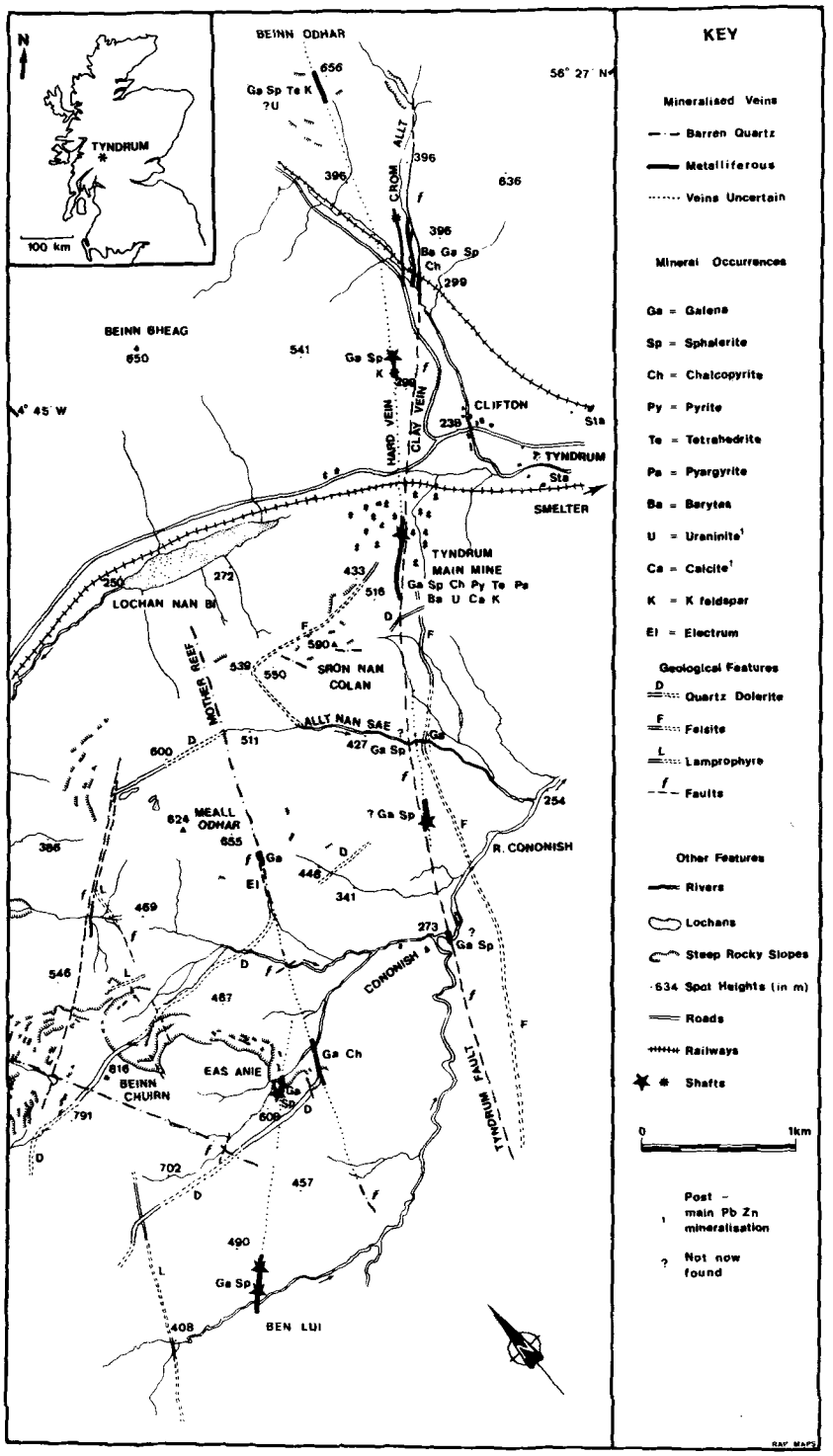

FIG. 1. The Tyndrum Mineral Veins.

Sulphide mineralogy. The breccias have variable mineralogies with different sulphide ratios and mineral relationships. The breccias can be broadly divided into five types: (i) Those comprising coarse-grained aggregates of sphalerite and acicular quartz with very minor amounts of galena, chalcopyrite, and pyrite, which represent the first stage of sulphide precipitation. (ii) Those consisting of equal volumes of coarse-grained (500 μm–2 cm) sphalerite and galena. Polished sections reveal the sphalerite to be slightly brecciated with quartz and galena occupying the fractures. (iii) Sulphide-rich injection breccias that comprise mixed aggregates of galena, sphalerite, fine-grained quartz, and minor amounts of chalcopyrite. Although the sphalerite is sometimes brecciated the minerals appear to have been co-precipitated. (iv) Quartz–galena breccias in which the galena grains (up to 5 cm across) have a cubic habit and are often associated with small (< 5 mm) irregular grains of chalcopyrite. (v) Rare samples of brecciated sphalerite cemented by quartz and chalcopyrite. The sphalerite is replaced along cleavages and grain boundaries by chalcopyrite which also forms blebs in the sphalerite.

There are vein-type ores with equivalent mineralogies to the breccias, although sometimes the vein-type ores contain more complex depositional sequences. Samples of vein ore with distinctive mineralogies were also recognized. These are: (i) Veins of quartz containing mainly galena and chalcopyrite which cut the quartz-sphalerite breccias. (ii) Rare quartz + chalcopyrite veins. (iii) The massive galena veins.

The veins of massive galena contain extensively replaced fragments of quartz and sphalerite. Polished sections reveal the galena to be a mosaic of interlocking grains (200 μm in diameter). Flame-shaped galena grains of slightly lower reflectance form rims around brecciated quartz fragments and may have developed during galena recrystallization, the resulting strain and lattice distortion adjacent to the inert quartz grains causing the lower reflectance. The galena contains very irregular grains and clusters of grains of chalcopyrite (20 μm to 1 cm across). Rare subhedral and anhedral marcasite grains (< 50 μm) are associated with the chalcopyrite. Both the chalcopyrite and marcasite are replaced at grain margins by galena, a process that appears to have taken place during post-depositional recrystallization. Euhedral pyrite grains (20–30 μm) often associated with chalcopyrite, occur in the galena. Euhedral quartz crystals (100 μm across) are common and small (< 80 μm) irregular grains of sphalerite also occur. Tetrahedrite grains (< 100 μm) are locally abundant occurring as euhedral crystals, irregular grains, graphic intergrowths with galena, and as cusp-shaped grains at triple junction grain boundaries in galena. The tetrahedrite is commonly associated with small chalcopyrite grains and more rarely with sphalerite and pyrite grains. Pyrargyrite grains (< 100 μm across) occur in the samples containing tetrahedrite and also form replacement rims around the tetrahedrite. One grain of pyrargyrite is intergrown with a bluish-green isotropic phase of slightly lower reflectance. Calcite is occasionally present in a few samples either as rhombs (20 μm) or irregular veinlets associated with chalcopyrite.

Microprobe analyses of tetrahedrite were briefly discussed by Pattrick (1978). The tetrahedrites are all silver-rich containing 6.6–30.9 wt. % Ag, this highest value being equivalent to 5.6 atoms Ag per $\frac{1}{2}$ unit cell. Riley (1974) termed tetrahedrites with more than 4 atoms Ag per $\frac{1}{2}$ unit cell (*c.*12 at. %) freibergites, although others (viz. Fleischer, 1975) suggest this name should be used for tetrahedrites with Ag > Cu. Riley's suggestion is based on an observed 'collapse' in cell size at > 4 atoms Ag; an observation supported by Petruk (1971) and Pattrick and Hall (1983). As Ag > Cu is an arbitrary boundary, Riley's usage is justified and thus some of the tetrahedrites are strictly freibergites.

Some inclusions of the tetrahedrite displayed distinct colour zoning with greenish-grey margins and grey higher reflectance cores. Different substitutions into tetrahedrites can affect the reflectance but microprobe analyses Ty 22A and D of the core and Ty 22B and C of the rim (Table I) show no consistent chemical variation. The colour variation may therefore reflect some slight structural variation in the tetrahedrites supported by observation that the margins have microfractures and the cores do not.

Microprobe analyses of pyrargyrite (analyses Pya-1 to 3, Table II) confirm its optical identification and show that some Cu is substituting for Ag. The pyrargyrite intergrown with a darker phase (analysis Pya-3) contains 2.50 wt. % Cu. The darker phase (phase *x*), however, contains *c.*8.0 wt. % Cu (analyses Px-4 to 7) but is not simply Ag_3SbS_3 with a greater Cu substitution, as recalculation, using S = 3, shows it to be Sb_2S_3-rich. Its apparent composition is closer to $5(Cu,Ag)_2S{\cdot}2Sb_2S_3$, although there is no recorded natural or synthetic phase of this composition. Cambi *et al.* (1966), in an experimental study of the join 3.5 $Cu_2S{\cdot}Sb_2S_3$–Ag_2S do, however, record a metastable stephanite at 60 wt. % Ag_2S, which is close in composition to 'phase *x*' though relatively Cu-poor. Close examination of the phase by SEM appears to confirm phase *x* to be homogeneous and not an intergrowth. Microprobe analyses of the sphalerite (from all localities) revealed iron contents in the range 9000–3000 ppm and cadmium concentrations of *c.*4500 ppm.

TABLE I Microprobe analyses from an optically zoned tetrahedrite (wt. %)*

Inclusion No.	Cu	Ag	Zn	Fe	Cd	Sb	As	S	Total
TY 22D	23.71	14.95	0.16	0.14	11.88	26.54	0.63	21.50	99.51
TY 22A	23.67	14.81	0.15	0.13	11.74	26.70	0.54	21.56	99.30
TY 22C	24.57	15.75	0.52	0.19	11.47	26.55	0.60	21.80	101.45
TY 22B	24.65	13.70	0.45	0.16	11 52	27.10	0.50	21.63	99.71

Analyses recalculated to tetrahedrite formula assuming $M^{+} + M^{2+} = 12$ in $(Cu,Ag)_{10}(Zn,Fe,Cd)_2(Sb,As)_4S_{13}$

TY 22D	7.195	2.672	0.047	0.048	2.038	4.203	0.162	12.928
TY 22A	7.223	2.662	0.044	0.045	2.025	4.252	0.140	13.037
TY 22C	7.182	2.712	0.148	0.063	1.895	4.050	0.149	12.627
TY 22B	7.423	2.430	0.132	0.055	1.961	4.259	0.128	12.907

*Wavelength Dispersive Analysis

Textural development in the massive galena veins. The textures observed in the massive galena veins formed by a process of recrystallization, exsolution, and solid state migration. Initially, the galena precipitated, together with minor amounts of other sulphides, from lead-rich solutions. During ensuing cooling and recrystallization the low solubilities of metals (including Ag and Sb) in galena at low temperatures would have led to the exsolution of further sulphide phases. In annealing experiments Amcoff (1976) demonstrated the exsolution of sulphides from galena with decreasing temperature and the appearance of more complex phases due to the reactivity of the sulphides and sulphosalts produced. The association between sulphides and some tetrahedrites in the vein galena is evidence that this type of reaction was involved in the formation of the Tyndrum tetrahedrites. Amcoff also observed the development of myrmekitic intergrowths and cusp-shaped inclusions of sulphosalts at grain boundaries. Both these features are present in the Tyndrum galena and are evidence of exsolution and migration to grain boundaries respectively.

Cadmium substitutes for Zn and Fe in the divalent site in some of the tetrahedrites analysed (see Table I) and was the first recorded occurrence of cadmium-tetrahedrite (Pattrick, 1978). As there is no evidence of an exceptionally high Cd content of the Tyndrum sphalerite a high Cd content in the mineralizing fluids cannot explain the unique substitution of Cd into tetrahedrites. A possible explanation, however, is the availability of elements during exsolution. The distribution of the highest silver and cadmium tetrahedrites (and pyrargyrite) in the Steel Ore galena is very irregular. This presumably represents the original distribution of minor elements during the precipitation of the galena which controlled the composition of the tetrahedrites formed during exsolution. There is a very strong fractionation of Cd towards sphalerite in sulphide assemblages (Bethke and Barton, 1971*a*) and in the presence of ZnS there may normally be little Cd available for substitution into tetrahedrite. However the samples containing high Cd-tetrahedrites contain no primary inclusions of sphalerite to 'soak up' the Cd. Bethke and Barton (1971*a*, *b*) determined the maximum solubility of Cd in galena to be 1500 ppm at 250 °C dropping to 300 ppm at 100 °C and also found rapid diffusion of Cd in galena in exsolution experiments. Therefore in the ZnS-free galena the Cd would exsolve, migrate, and react with other exsolving elements and compete for the divalent site in tetrahedrite.

Gangue minerals. Quartz is by far the predominant gangue mineral and precipitated throughout the whole mineralizing episode. It occurs as acicular crystals on vein margins and surrounding breccia fragments and as cryptocyrstalline silica in breccias rich in sulphides. Chert also occurs in the breccias, being interstitial to acicular quartz and usually rimmed by a band of sphalerite. Some samples of massive quartz comprise skeletal needle-like crystals (up to 4 cm in length) set in a mosaic of equigranular crystals. The cryptocrystalline and skeletal silica are indicative of periods of very fast precipitation from supersaturated solutions.

Odernheimer (1841) noted that schistose bands in the Eilde Flags were totally replaced by pink feldspar at their intersection with the Hard Vein and Halliday (1962) reported veins of quartz, feldspar, galena, and pyrite in core from holes drilled below the Main Mine. This evidence of the

close association of the K-feldspar to the Hard Vein has been destroyed by mining operations but some dump samples contain pink feldspar crystals (up to 3 cm across) associated with quartz and sulphides. Thin section observations and X-ray diffraction analysis revealed two intergrown K-feldspars; microcline and orthoclase. These K-feldspars are often slightly brecciated and must have formed in an early stage of the mineralizing episode.

Massive white baryte is a minor constituent of the ore in the Main Mine.

During the main sulphide precipitation carbonate was a very minor phase. There are, however, a number of dump samples comprising coarse crystalline pink calcite forming the matrix in a breccia of green-stained (chloritized) quartzite fragments. Fragments of the main Pb–Zn mineralization are included in these breccias. Pink calcite is associated with rebrecciation of quartz–sulphide veins and breccias; calcite veins up to 2 cm across also cut sulphide-bearing veins. The presence of pink calcite suggests that this phase of the mineralization may be related to the uranium-bearing mineralization (see below).

The late uraniferous mineralization. A small but distinct mineralization of different character to the main mineralization has been recognized in the Maine Mine. A dump specimen of 'pitchblende' with calcite, baryte, and chalcopyrite was the subject of an age-dating study (Darnley *et al.*, 1960) and further investigation uncovered a small veinlet of 'uraninite' in a level driven 300 m into the hillside in 1925 (Darnley, 1962). The pitchblende is associated with coarsely crystalline pink calcite, which owes its colour to inclusions of hematite, and the uraninite is associated with sulphides occupying vuggy cavities. The mineralogy recorded was chalcopyrite, pyrite, marcasite, galena, and safflorite associated with secondary erythrite, zeunerite, and the uranium minerals uranospinite, kasolite, and liebigite. The veinlet trends NW–SE and postdates the main sulphide mineralization. In the Beinn Odhar level, uranium minerals were identified in a similar cross-fracture (Harrison, 1956).

The 1925 level is closed by a rockfall but two dump samples of uranium ore were studied in polished section and revealed a complex mineralogy and depositional sequence. Examination of the first sample revealed that the first deposited minerals were quartz, dolomite and K-feldspar. These minerals were extensively replaced by later carbonates and sulphides. Sphalerite (see Table III) was the first sulphide deposited and is replaced along grain margins by chalcopyrite and along fractures by galena. Uraninite was the next mineral deposited forming collomorphic bands and irregular grains (fig. 2). The uraninite contains many inclusions of galena and is also replaced by chalcopyrite and galena. A second uraninite generation is represented by radiating aggregates of needles and is associated with pink calcite and chalcopyrite with minor quartz, pyrite, galena and small (*c.*15 μm) grains of native copper and silver, argentite, and argentian chalcocite. A late galena generation replaces sphalerite and chalcopyrite and contains small (*c.*10 μm) inclusions of tetrahedrite (Table III).

The second sample contains fragments of quartz–chlorite schist which have been extensively replaced by later sulphides and carbonate. Deposition of pink baryte (with hematite inclusions) was followed

Table II Average microprobe analyses of Pyrargyrites (Pya-1 to 3) and Phase x (Px-4 to 7) intergrown with Pyrargyrite (Pya-3).

	Cu	Ag	Zn	Cd	Sb	As	S	Total
Pya-1	0.72	57.49	0.02	0.00	24.51	0.00	18.10	100.84
Pya-2	1.29	58.32	0.00	0.00	23.46	0.00	17.15	100.22
Pya-3	2.50	57.04	0.00	0.00	23.68	0.37	17.98	101.57
Px-4	8.20	44.74	0.20	0.71	26.64	0.05	20.10	100.64
Px-5	7.83	43.77	0.20	0.58	27.57	0.00	20.04	99.98
Px-6	8.41	43.13	0.43	0.97	27.36	0.30	20.94	101.54
Px-7	8.52	45.26	0.00	0.53	27.43	0.13	20.34	102.21

Analyses recalculated assuming S = 3

		Cu	Ag	Zn	Cd	Sb	As	S
Pya-1	Pyrargyrite	0.06	2.83	0.00	0.00	1.07	0.00	3.00
Pya-2	Pyrargyrite	0.11	3.03	0.00	0.00	1.08	0.00	3.00
Pya-3	Pyrargyrite	0.21	2.83	0.00	0.00	1.04	0.03	3.00
	Phase x	0.62	1.99	0.02	0.03	1.05	0.00	3.00
	Phase x	0.52	2.06	0.00	0.03	1.07	0.00	3.00
	Phase x	0.61	1.84	0.03	0.04	1.03	0.02	3.00
	Phase x	0.63	1 98	0.00	0.02	1.07	0.01	3.00

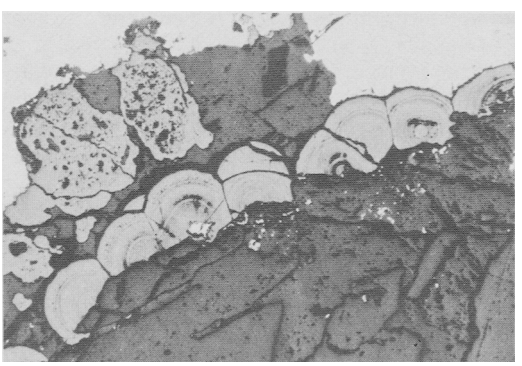

FIG. 2. Colloform and massive uraninite (grey), carbonates (black) and galena (white) from Tyndrum Main Mine.

Table III Representative microprobe analyses of minerals associated with the uraniferous mineralization (wt. %)*

		Cu	Ag	Co	Zn	Fe	Cd	Sb	As	S	Total
Tu-1	Silver	0.13	99.90	0.03	0.00	0.00	0.00	0.00	0.04	0.06	100.16
Tu-2	Chalcocite	70.57	5.31	0.02	0.07	0.00	0.25	0.00	0.10	22.03	98.35
Tu-3	Argentite	0.05	86.38	0.00	0.00	0.00	0.00	0.00	0.32	14.40	101.15
Tu-4	Tetrahedrite	33.87	2.08	0.00	6.96	0.24	0.25	29.25	1.80	24.03	98.48
Tu-5	Tetrahedrite	34.36	2.24	0.33	6.91	0.33	0.00	29.11	1.62	24.22	99.12
Tu-6	Tetrahedrite	34.38	1.79	0.00	7.14	0.22	0.19	29.23	1.40	24.16	98.51
Tu-7	Sphalerite	0.00	0.00	0.00	66.43	0.79	0.27	0.02	0.03	32.31	99.85
Tu-8	Safflorite	0.71	0.00	28.27	0.00	0.59	0.00	0.00	71.15	0.34	101.06
Tu-9	Safflorite	0.00	0.00	29.93	0.00	0.56	0.00	0.00	70.33	1.00	101.82

		UO_{2+x}	PbO_2	Fe_2O_3	MnO	CaO	P_2O_5	SiO_2	Total
Tu-10	Uraninite	86.78	9.86	0.05	0.22	2.43	0.00	2.22	101.56
Tu-11	Uraninite	87.34	8.38	0.00	0.00	3.82	0.00	2.30	101.84
Tu-12	Uraninite	89.97	1.08	0.89	0.78	4.34	0.00	3.90	100.96
Tu-13	Uraninite	85.89	2.24	0.70	0.42	4.52	1.16	3.41	98.34
Tu-14	Uraninite	86.25	2.29	0.74	0.42	4.05	0.94	3.70	98.39

* below detection limit: Zr, Th, S, Pr & Ce.

by two generations of calcite. The first, a pink variety, contains inclusions (< 500 μm) of hematite, chalcopyrite, and pyrite, while the second is associated with chalcopyrite (grains up to 1 cm) and some subhedral pyrite, as well as rare irregular inclusions of Co-rich safflorite (Table III). Sphalerite and galena are also present, replacing the chalcopyrite. The uraninite was late in the paragenetic sequence, often occurring as bands (up to 200 μm across) of anhedral and acicular crystal aggregates intergrown with calcite and surrounding the chalcopyrite grains. Sometimes larger (3 mm) irregular aggregates of uraninite have developed in the calcite.

Microprobe analyses of the uraninite from both samples (Table III) reveal no detectable Th or *REE*, a common feature of the pitchblende variety (Steacy and Kaiman, 1978), but significant concentrations of SiO_2 and CaO. Frondel (1958) suggested that SiO_2 in uraninite analyses is due to impurities, although the consistency of the concentrations of CaO and SiO_2 and the lack of visible inclusions indicate them to be substituting in the uraninite. Ludwig and Grauch (1980) record a similar consistency of CaO and SiO_2 concentration in uraninite, explaining the CaO substitution by the similar ionic radii of U^{4+} and Ca^{2+}, although the substitution of Si^{4+} is more difficult to justify. The high PbO_2 values in the analyses of the colloform uraninite (Tu-11 and 12) are probably due to inclusions; a large number are visible in polished section.

In his description of the mines, Odernheimer (1841) reports the occurrence in the Main Mine of a cobalt-rich vein, which yielded '25% cobalt and 60 oz/ton Ag', cross-cutting the Pb–Zn mineralization. A sample examined in this study showed it to comprise mainly erythrite and baryte fragments. As secondary erythrite was also reported in the only other uraninite locality, the Beinn Odhar Level (Harrison, 1956), it is possible that the cobalt enrichments are the result of weathering of the uraniferous veins.

Paragenetic sequence. Although the use of dump samples leads to many uncertainties concerning mineral relationships a general sequence of mineral formation can be deduced from the Tyndrum Main Mine samples described above and is shown in fig. 3.

Other localities

The Crom Allt veins consist of both breccia and vein ores. One vein displays several stages of mineralization; an initial minor quartz veining followed by brecciation and precipitation of quartz, coarse-grained galena, minor sphalerite, and chalcopyrite, then further brecciation and introduction of coarse-grained, bladed white baryte, and quartz with minor galena. In some places the vein-breccias are cut by baryte veins (*c.*4 cm wide) carrying galena and sphalerite and surrounded by a 'halo' of chalcopyrite grains (< 5 mm). Veins of massive baryte also occur as do veinlets of quartz with galena and chalcopyrite. Baryte is about 50% by volume of the Crom Allt veins. The quartzite breccia fragments and wallrocks in the Crom Allt veins are extensively replaced by silica and indigenous feldspars are altered to chlorite and sericite. Euhedral pyrite grains (*c.*100 μm) have developed in the quartzite.

Polished sections of an outcropping vein on Beinn Odhar reveal quartz containing slightly brecciated sphalerite, galena, and minor chalco-

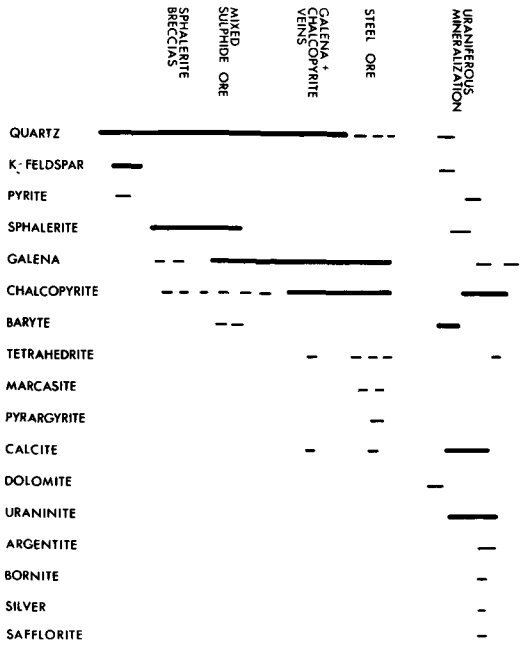

FIG. 3. Paragenetic sequence of mineralization in the Main Mine.

pyrite. The galena contains rare small (< 10 μm) tetrahedrite inclusions.

At Eas Anie the only mineralization remaining is in small veins (3 cm wide) of quartz + galena and quartz (displaying a cockscomb texture) + chalcopyrite.

The Ben Lui dumps consist of breccia-ores containing quartz, galena, and sphalerite with minor chalcopyrite. Examination of material from a trial into the Mother Reef (fig. 1) showed galena to be the only sulphide present. At the western margin of the Mother Reef on the southern slope of Meall Odhar (fig. 1) pyrite is present in fractures. This pyrite is associated with a fault parallel to the quartz vein. The fault plane is filled by clayey material and brecciated quartz. K-feldspar, albite, and minor rutile are present and the pyrite contains grains of electrum (< 20 μm), which have a composition *c.*Au_{53} to Au_{64}. The causes of this mineralization and its relationships with the Mother Reef and Pb–Zn veins are being investigated.

Fluid inclusion studies

Results. Fluid inclusions in sphalerite and quartz were studied to determine the nature of the mineralizing fluids. The temperatures and salinities of the fluids were investigated using a Linkham TH 600 heating stage; Na, Ca, and K ratios were determined by decrepitation of inclusions in bulk mineral samples.

Most of the fluid inclusions were too small to use but a few yielded important information which is summarized in fig. 4. One population of primary inclusions has consistent salinities around 18.0 wt. % equivalent NaCl. These inclusions yield T_h values ranging from 100 °C to > 400 °C. In two samples of quartz, inclusions in close proximity have very variable liquid–vapour ratios giving a range of T_h from 153 °C to > 400 °C. In some quartz samples there are two types of inclusion; one with high salinity having small or no vapour bubbles and the other very vapour-rich (the latter cannot be plotted on fig. 4). In the absence of evidence of necking, in most cases, these features of the inclusions are evidence for crystal growth from a boiling solution (Roedder and Bodnar, 1980). The non-saline fluid inclusions are interpreted as representing condensate resulting from boiling. Inclusions from the Mother Reef indicate that it formed from a different mineralizing fluid of lower salinity which was not boiling (fig. 4).

The decrepitation experiments on bulk samples of quartz and sphalerite produced low concentrations of dissolved species, a consequence of poorly developed primary fluid inclusions. Na/K ratios derived from seven quartz samples averaged 2:1 and five sphalerite samples, 4:1. These ratios imply a high concentration of KCl in the fluids and therefore the estimated salinity of the mineralizing fluid must be revised to approximately 20 wt. % NaCl + KCl; see fig. 4.

Discussion. The Na/K ratios are significantly low for hydrothermal Pb–Zn deposits and cannot be explained by a genetic association with acid intrusives (Rye and Haffty, 1969), interaction with evaporites (White *et al.*, 1963), or by rock–water reactions at high temperatures (Orville, 1963; Hemley and Jones, 1964). The country rocks beneath Tyndrum, however, are Dalradian and Moinian garnet–mica schists and feldspathic quartzites with higher grade quartzo-feldspathic metamorphics at depth. These lithologies are high in potassic minerals and Ellis (1979) noted that fluids reacting with these rocks would evolve a low Na/K ratio.

The temperature of the boiling mineralizing fluids cannot be determined accurately although it was probably in the range 140–250 °C (fig. 4). Fluids of this temperature and salinity (20 wt. %) would have been capable of carrying up to 100 ppm Pb and higher concentrations of Zn. The consequences of boiling of mineralizing fluids have been summarized by many authors (e.g. Barton *et al.*, 1977; Ellis and Mahon, 1977; Bush, 1980; and

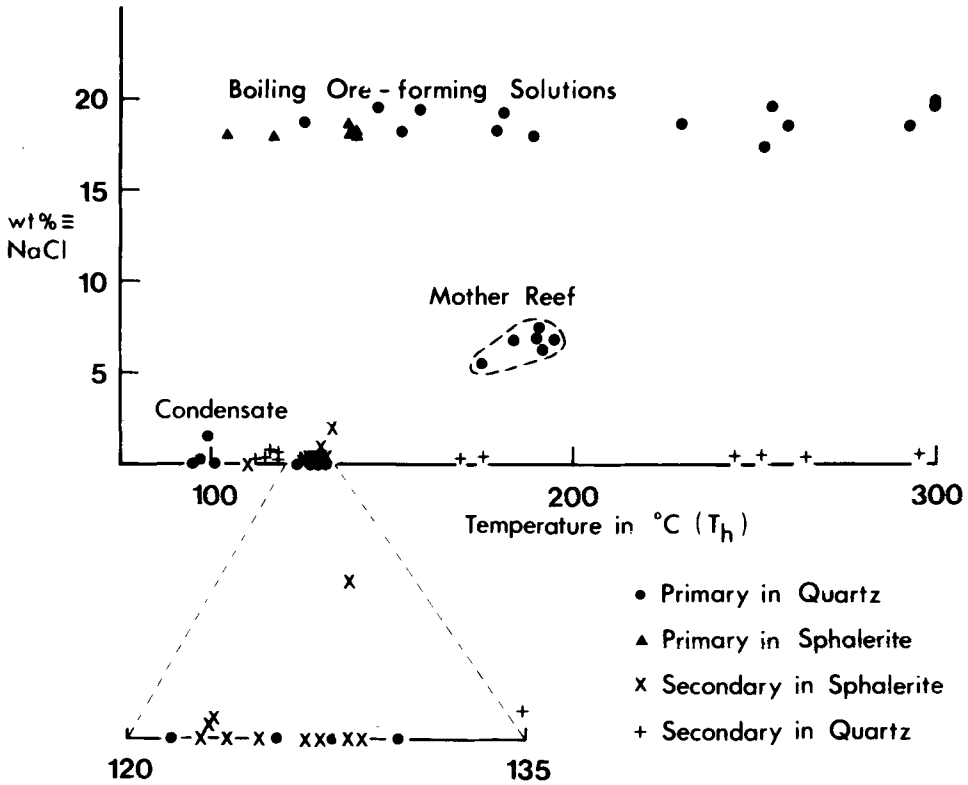

FIG. 4. Summary of fluid inclusion data from Tyndrum Hard Vein minerals. (Including a few analyses from the Mother Reef for comparison.)

Arnorsson, 1978) and include: (*a*) a sudden temperature drop due to enthalpy loss to evolved steam, (*b*) a pH rise due largely to CO_2 loss in the vapour phase and the loss of H_2S, (*c*) the formation of an acidic low salinity condensate. The pH rise and temperature fall result in a great reduction in metal solubilities and this boiling was probably a major mechanism of mineral precipitation in the Tyndrum Mines. Other factors causing mineral precipitation could have been the general cooling of the rising hydrothermal fluids and mixing with meteoric water. Sulphur isotope data indicate mixing in the upper levels of the veins (Pattrick *et al.*, 1983).

The high K^+ concentration and boiling of the mineralizing fluids could explain the occurrence of K-feldspar as a product of wallrock alteration (Brown and Ellis, 1970; Steiner, 1970).

Discussion of the vein evolution

The Tyndrum fault, acting as a relatively high permeability zone, was the major control on the rising hydrothermal fluids. These fluids migrated into the fault plane at depth and mineral precipitation here was limited because the fluids rose under pressure and at high velocity (Ellis, 1979). The most significant mineralization took place where the fluids passed into permeable fractures in competent quartzites that intersect the fault, such as the Crom Allt veins (fig. 1).

The initial development of the Hard Vein and Tyndrum breccias can be explained by processes similar to those evoked by Philips (1972) for the Central Wales Pb–Zn veins with brecciation and mineralization occurring during the extension of pre-existing faults as the result of a build up of hydrostatic pressure. At Tyndrum, fluid in the fault plane was forced into the Hard Vein fracture and its adjacent pore spaces and joint planes. If the pressure of the hydrothermal solution in the Hard Vein was sufficiently higher than the prevailing pore pressure, then fracturing would be the result. Fluid in the local pore space moving into the resulting low-pressure zone would fragment the rocks, a process enhanced by the separation of a gas

phase or water vapour as the pressure dropped. Henley (1973) explains the formation of breccia pipes in the same manner with fluid building up until $P_{H_2O} \gg P_{load}$ leading to fracturing on a plane of weakness. Brecciation by this mechanism could have developed the Hard Vein fracture into a highly permeable channelway for solutions and could have caused its extension towards the surface, possibly with the formation of a 'hot spring' outlet for the solutions. The Hard Vein would then have become a potential site for continuing mineralization, fluids tapped from the fault plane would have a lower velocity in the more permeable, smaller Hard Vein, thus encouraging mineral precipitation.

The hydraulic and intrusion breccia development was related to fluid velocity; intrusion breccias formed in the centre of the vein where velocities were high enough to move small fragments in relation to each other and hydraulic breccias formed where no movement took place, on the outside of the veins (Philips, 1972; Raybould, 1974). Chemical brecciation (Sawkins, 1969) may have been an important process in continuing the vein expansion with crystal growth and chert precipitation developing and enlarging the breccias.

Some of the vein ores developed where solutions exploited small linear fractures in the quartzite. The veins cutting the breccias, however, could have formed because of linear fracturing related either to fluid pressure build up during temporary sealing of the vein or to stresses resulting from crystallization.

The Crom Allt veins probably have a similar origin to the Hard Vein. The other metalliferous mineralized localities (fig. 1) are not so obviously related to the Tyndrum fault but their similar mineralogies and textures suggest they were formed in the same hydrothermal event. These mineralized fractures may connect with the fault plane at depth, the distance from the fault explaining the paucity of mineralization. The Mother Reef (fig. 1) is a zone of intense silicification with little metalliferous mineralization formed by a more passive injection of mineralizing solutions. Fluid inclusion data suggest this may have been a different mineralizing event.

Modelling of the chemical evolution of the system is restricted because of the lack of *in situ* material and of well-defined chemical conditions of ore formation. Any model should explain the general sequence $ZnS \rightarrow PbS + CuFeS_2 \rightarrow UO_2 + CuFeS_2$.

Samples of breccias formed during periods of fast precipitation contain co-precipitated ZnS, PbS, and $CuFeS_2$ showing that the early mineralizing fluids carried significant concentrations of both Zn and Pb (in a ratio 4 : 1) and small concentrations of Cu and Fe. The relationships observed in many of the early breccias however revealed the sequence sphalerite then galena. This sequence may have developed when precipitation rates were slow and a solution of the inferred metal ratios would have precipitated ZnS at lower levels in the vein than PbS (see Sato, 1973).

The later $PbS + CuFeS_2$ stage of mineralization can be explained by an increase in mineralizing fluid temperatures with time, combined with a change in source rocks. Such conditions would be found in the downward penetrating convection systems that Russell (1978, 1983) evokes for sediment-hosted exhalative Pb–Zn deposits. In such a system at Tyndrum early, lower-temperature (*c.*150 °C) fluids circulating at shallow levels (< 5 km) would encounter mainly garnet pelites containing very approximately 140 ppm Zn, 40 ppm Pb, and 65 ppm Cu (Senior and Leake, 1978). The solutions would become reduced and acid by rock–water reaction (Russell *et al.*, 1981) and leach out metals thus deriving a high Zn : Pb ratio. These solutions would be too cool to carry much Cu. As fluids reached deeper levels they would encounter more quartzo-feldspathic rocks (Richardson and Powell, 1976) containing higher levels of Pb and lower levels of Zn and Cu [50 ppm, 20 ppm, and 14 ppm respectively in K-feldspar gneiss (Senior and Leake, 1978)]. These solutions would attain higher temperatures (300 °C at 10 km assuming a geothermal gradient of 30 °C/km) and would evolve high Pb : Zn ratios and be hot enough to carry Cu in solution (Crerar and Barnes, 1976). The early fluids in this model would precipitate the Zn-rich breccias. The later fluids, being hotter, would boil at lower levels in the vein system causing linear brecciation and replacement of earlier breccias and precipitation of $PbS + CuFeS_2$-rich veins.

It is not certain that the uraniferous mineralization was formed by the same hydrothermal event as the main sulphide mineralization. However, the solutions that caused the uraniferous mineralization would have had a relatively high f_{O_2} and f_{CO_2}, the uranium travelling as U^{6+} in hydroxyl and carbonate complexes (Rich *et al.*, 1977; McLennan and Taylor, 1979). These high Eh solutions with a high $\Sigma SO_2/H_2S$ ratio would favour Cu transport and precipitate sulphates. Such solutions could have evolved late in the cooling stage of the Tyndrum hydrothermal system (see Russell and Samson, 1982; Russell, 1983) because the removal of Mg by wallrock reaction, which is the main mechanism for sulphate removal and the decrease in pH in heated mineralizing fluids, will have ceased due to the replacement of all available soluble

cations in the channeleway wallrocks (Bischoff and Seyfreid, 1978; Seyfreid and Bischoff, 1979). This process would be effective at Tyndrum because fluid flow through the meta-sedimentary country rocks would be in a fracture controlled system with a high water-rock ratio. Alternatively the uraninite mineralization could have resulted from a later unrelated hydrothermal event. For instance, Davidson (1966) suggested the involvement of downward percolating saline groundwater of Triassic red-bed origin. These solutions could have precipitated U and Cu on being reduced by reaction with the existing sulphides. The suite of secondary minerals with the uraninite are consistent with post-depositional oxidation (Frondel, 1958) which would also account for the erythrite-rich veins.

The fundamental causes of the Tyndrum mineralization and the relationship between the Pb-Zn and U stages are not obvious from the field relationships and mineralogy. The understanding of these are the subject of a K-Ar, Rb-Sr, and Sr^{86}/Sr^{87} study on the K-feldspar, sulphates, and carbonates.

Acknowledgements. The author is greatly indebted to Dr A. J. Hall and Professor M. J. Russell for assistance and discussions during this study. Dr W. E. Stephens is thanked for initial encouragement and John Burton of Cononish and the Forestry commision are thanked for access to the mines. Dr P. J. Hill, D. A. Plant, and T. C. Hopkins are gratefully acknowledged for help with the microprobe analyses. P. Duller and the Royal Scottish Museum are thanked for providing the samples of uranium ore. The author is grateful to D. A. Polya, R. A. Scott, and C. Dickinson for critically reading the manuscript. The work was undertaken as part of a NERC research studentship at the University of Strathclyde. Microprobe analyses were performed on NERC supported microprobes at the Universities of Edinburgh and Manchester.

REFERENCES

Amcoff, O. (1976) *Neues Jahrb. Mineral. Mh.* 247–61.
Arnorsson, S. (1978) *Contrib. Mineral. Petrol.* **66,** 21–8.
Barton, P. B., Bethke, P. M., and Roedder, E. (1977) *Econ. Geol.* **72,** 1–25.
Bethke, P. M., and Barton, P. B., (1971*a*) Ibid. **66,** 140–63.
——— (1971*b*) *Am. Mineral.* **56,** 2034–9.
Bischoff, J. L., and Seyfreid, W. E., Jr. (1978) *Am. J. Sci.* **278,** 838–60.
Brown, P. R. L., and Ellis, A. J. (1970) Ibid. **269,** 97–131.
Bush, P. R. (1980) 4th Australian Geological Congress, Hobart; Abstracts. Geol. Soc. Austral. 5.
Cambi, L., Elli, M., and Tangerini, I. (1966) *Chim. Ind. (Milan),* **48,** 567–75.
Crerar, D. A., and Barnes, H. L. (1976) *Econ. Geol.* **71,** 772–94.
Darnley, A. G. (1962) Geol. Surv. GB *Age Determination Report,* 21.
—— Smith, G. H., Chandler, T. R. D., and Preece, E. R. (1960) Geol. Surv. G.B. *Age Determination Report,* 13.
Davidson, C. F. (1966) *Trans. Inst. Mining Metall.* B, **75,** 237–41.
Ellis, A. J. (1979) *Chem. Geol.* **25,** 219–26.
—— and Mahon, W. A. J. (1977) *Chemistry and Geothermal Systems.* Academic Press, Inc. 392 pp.
Fleischer, M. (1975) *Am. Mineral.* **60,** 489.
Frondel, C. (1958) *Systematic mineralogy of uranium and thorium.* US Geol. Surv., Bulletin 1064.
Halliday, L. B. (1962) Reports of Surveys at Tyndrum. On file at IGS, Edinburgh.
Harrison, R. K. (1956) *Report on the preliminary survey of radioactivity in the Tyndrum mining area.* Geol. Surv. GB Atomic Energy Division, Report No. 186.
Hemley, J. J., and Jones, W. R. (1964) *Econ. Geol.* **59,** 539–67.
Henley, R. W. (1973) *Trans. Inst. Mining Metall.* B, **82,** 1–8.
Ludwig, K. Z., and Grauch, R. I. (1980) *Econ. Geol.* **75,** 296–302.
McLennan, S. M., and Taylor, S. R. (1979) *Nature,* **282,** 247–50.
Odernheimer, F. (1841) *Trans. Highland Soc.* **7,** 541–56.
Orville, P. M. (1963) *Am. J. Sci.* **261,** 201–37.
Pattrick, R. A. D. (1978) *Mineral Mag.* **42,** 286–8.
——(1981) *The vein mineralization at Tyndrum, Scotland, and a study of substitutions in tetrahedrites.* Ph.D. thesis, University of Strathclyde.
—— and Hall, A. J. (1983) *Mineral. Mag.* **47,** 441–51.
—— Coleman, M. L., and Russell, M. J. (1983) *Mineral. Deposita.* **18,** 477–85.
Petruk, W. (1971) *Can. Mineral.* **11,** 196–231.
Philips, W. J. (1972) *J. Geol. Soc. Lond.* **128,** 337–55.
Raybould, J. G. (1974) *Trans. Inst. Mining Metall.* B, **88,** 112–19.
Rich, R. A., Holland, H. D., and Petersen, U. (1977) *Hydrothermal Uranium Deposits.* Elsevier, 264 pp.
Richardson, S. W., and Powell, R. (1976) *Scott. J. Geol.* **12,** 237–68.
Riley, J. F. (1974) *Mineral Deposita.* **9,** 117–24.
Roedder, E., and Bodnar, R. J. (1980) *Ann. Rev. Earth Planet. Sci.* **8,** 263–301.
Russell, M. J. (1978) *Trans. Inst. Mining Metall.* B, **87,** 167–71.
——(1983) In *Sediment Hosted Stratiform Lead-Zinc Deposits* (D. F. Sangster, ed.). Short Course Handbook **8,** MAC, 251–82.
—— and Samson, I. M. (1982) MDSG Meeting, University of Strathclyde, Abstracts, 4.
—— Solomon, M., and Walshe, J. L. (1981) *Mineral. Deposita.* **16,** 113–27.
Rye, R. O., and Haffty, J. (1969) *Econ. Geol.* **69,** 468–81.
Sato, T. (1973) *Geochem. J.* **7,** 245–70.
Sawkins, F. J. (1969) *Econ. Geol.* **65,** 613–17.
Senior, A., and Leake, B. E. (1978) *J. Petrol.* **19,** 584–825.
Seyfreid, W. E., Jr., and Bischoff, J. F. (1979) *Geochim. Cosmochim. Acta,* **43,** 1937–49.

Steacy, H. R., and Kaiman, S. (1978) In *Uranium Deposits. Their Mineralogy and Origin* (M. M. Kimberley, ed.). Short Course Handbook, **3**, MAC 107–39.
Steiner, A. (1970) *Mineral. Mag.* **37**, 916–22.
Thost, C. H. G. (1860) *Proc. Geol. Soc.* 421–8.
White, D. E., Hern, J. D., and Waring, G. A. (1963) *U.S. Geol. Surv. Prof. pap.* 440-F.
Wilson, G. V., and Flett, D. S. (1921) *The lead, zinc, copper and nickel ores of Scotland.* Mem. Geol. Surv. Scotland. Special Report on the mineral resources of Great Britain, 17.
Wilson, J. S. G., and Cadell, M. (1884) *R. Phys. Soc. Edinb.* **8**, 189–207.

[*Manuscript received 25 May 1984; revised 31 January 1985*]